Neural spike sorting using iterative ICA and deflation based approach

Z. Tiganj[1] **and M. Mboup**[2,3]

[1] LISV, University of Versailles Saint-Quentin-En-Yvelines, Velizy, France
[2] CReSTIC, University of Reims Champagne Ardenne, BP 1039 Moulin de la Housse, Reims, France
[3] Non-A, INRIA Lille - Nord Europe, Villeneuve d'Ascq, France

E-mail: `zoran.tiganj@gmail.com`, `Mamadou.Mboup@univ-reims.fr`

Abstract. We propose a spike sorting method for multi-channel recordings. When applied in neural recordings, the performance of the Independent Component Analysis (ICA) algorithm is known to be limited, since the number of recording sites is much lower than the number of neurons. The proposed method uses an iterative application of ICA and a deflation technique in two nested loops. In each iteration of the external loop, the spiking activity of one neuron is singled out and then deflated from the recordings. The internal loop implements a sequence of ICA and sorting for removing the noise and all the spikes that are not fired by the targeted neuron. Then a final step is appended to the two nested loops in order to separate simultaneously fired spikes. We solve this problem by taking all possible pairs of the sorted neurons and apply ICA only on the segments of the signal during which at least one of the neurons in a given pair was active. We validate the performance of the proposed method on simulated recordings, but also on a specific type of real recordings: simultaneous extracellular-intracellular. We quantify the sorting results on the extracellular recordings for the spikes that come from the neurons recorded intracellularly. The results suggest that the proposed solution significantly improves the performance of ICA in spike sorting.

1. Introduction

Information between neurons is transmitted using electrochemical signaling, which includes communication through action potentials (AP).

Multi-site electrodes with an increasing number of channel recordings are being more and more used for accessing neural activity (see, e.g., [1] where 100-channels recording system, described in [2], has been used). Each recording site will capture a mixture of activities from a number of neurons around.

Finding the firing instants of individual neurons form extracellular recordings is a very challenging problem in neuroscience, known as spike sorting (when recorded with extracellular electrodes action potentials are usually called spikes). For reviews and comparison of the existing spike sorting methods, we refer to [3], [4] and [5] to name a few.

A preliminary step before actually sorting the spikes is to find and extract them from the original noisy measurement. This is the *spike detection* problem. For recordings with good Signal to Noise Ratio (SNR) spike detection can be solved by a simple thresholding [6]. When the SNR is not good enough, different spike detection algorithms can be applied, e.g.: [7], [8] and [9]. In general, only spikes with high enough amplitude can be detected. These correspond to the activity of the neurons closest to the recording sites. We mention however that, since the medium around the electrodes is not isotropic in general, the term *closest* does not always translate in the sense of minimum distance. So here and in all the remaining, *closest neurons* means neurons that are most visible in terms of current flow at the recording points during APs. The cumulative activity of all remote (in the sense above) neurons is considered as an undesired perturbation in the recorded signal, forming the background noise. And even for the neurons close to the electrodes, not all of their spikes are detected: some are inevitably lost due to the background noise corruption. However, analyzing the performance in spike sorting, we can say that missing some spikes (not detected spikes or spikes left unsorted) is less problematic than assigning spikes into a wrong cluster. We refer to [10] for detailed argumentation of this statement.

Commonly, spike sorting techniques use spike shape and amplitude as discriminative factors: even though all the neurons fire almost the same action potential waveform, due to the propagation and the velocity effects, spikes recorded with an extracellular electrode have different shapes and amplitudes if they are coming from different neurons [11]. Thus, after spike detection, feature extraction techniques such as Principal Component Analysis (PCA) [12], wavelet based feature extraction [13], [14] or some others [15], [16] are commonly applied on the detected spikes.

Spikes are then sorted into different clusters, depending on the extracted features. A large number of clustering algorithms have been proposed for spike sorting. K-means [17], EM [18], template matching [19], Bayesian clustering [20] and super-paramagnetic clustering [13] are just some popular/recent examples. The number of clusters is often determined manually. However, sometimes some unsupervised procedures are used. As

examples we mention Basysian Information Criterion (BIC) (e.g. [21] and [22]) as well as some simple ad-hoc procedures, such as finding the maximal density of the spikes in the feature vector space [23]. The essential problem in spike sorting arises from the fact that the activities of neurons close to the electrode are often significantly destroyed by the background noise. Thus, very often different spikes fired by the same neuron appear in a recording as very different waveforms and it is very hard to recognize that they should be sorted into the same cluster.

In multi-channel (multi-site) recordings, the activity of each neuron in the neighborhood is captured by several recording sites. The principle of many spike sorting algorithms is to exploit such information redundancy. This is actually a Blind Source Separation (BSS) problem which is commonly approached via Independent Component Analysis (ICA). It allows one to find a new basis of data representation in which the mutual information between the induced virtual recording sites is minimized [24], [25], [17] and [26]. For further reading, we refer to [27] for a nice tutorial on ICA (see also [28]). Unfortunately, the contribution of ICA is limited by several characteristics of neural recordings. The foremost is that the number of electrodes is much smaller than the number of neurons around. Also, the activities of different neurons are not independent. Consequently, ICA alone can not fully separate neural activities, but it can often transform the recorded signal so that the sorting is easier. Thus in general ICA is followed by some classical spike sorting algorithm (such as those we have mentioned in the previous paragraph).

In this paper we present a new algorithm for spike sorting from multi-channel extracellular recordings. The algorithm is iterative and consists of two nested loops. We use a deflation technique to improve the performance of ICA: after we separate the firing instants of a single neuron (using ICA and some spike sorting method), we remove them from the original recording and repeat the procedure until the algorithm becomes unable to separate any more neurons or until a prescribed number of neurons is obtained. Moreover, within each iteration we implement, in an internal loop, another iterative algorithm for removing the noise and all the spikes that are not coming from the neuron which is the closest to (the most visible by) the electrode. This neuron is identified as the one whose activity has the largest projection on the recording sites.

More precisely, the iteration of the internal loop consists of a sequence of ICA, and spike sorting. For the classical sorting algorithm we devised a simple greedy method, described in [23]. The algorithm is based on the observation that the distribution of a neural signal deviates significantly from the uniform distribution and is rather unimodal. The detected spikes to be sorted are first processed with some feature extraction technique and then represented in a space with reduced dimension by keeping only a few most important features. The resulting space is next filtered in order to emphasis the differences between the centers and the borders of the clusters. Using some prior knowledge on the lowest level activity of a neuron, as, e.g., the minimal firing rate, we find the number of clusters and the center of each cluster. The spikes are then sorted using a simple greedy algorithm which grabs the nearest neighbors. This

sorting method is selected for two reasons: 1) It does not require manual supervision, which would not be suited for an iterative algorithm. 2) It gives a good measure of distance between the clusters which, as we will see later, helps to determine which spikes can be deflated.

At the end of the external loop, we sort the overlapped spikes. This is done by taking all the possible pairs of the separated neurons and applying ICA only on the segments of the signal during which at least one of the neurons in a given pair was active.

The paper is organized as follows. In section 2 we describe two types of signal that we use in the simulations to come: 1) An artificially created neural mixture, where we simulate a four-channel extracellular recording in population of 1000 neurons distributed around the electrode. 2) A real simultaneous intracellular-extracellular recording [11] - we test the sorting algorithms on the extracellular recording and use the intracellular to verify the results for the intracellularly recorded neuron. In section 3 we give a step-by-step description of the proposed algorithm. In section 4 we give the complete results of the simulations for each step of the proposed algorithm. Concluding discussion is given in section 5.

2. Simulation settings

In this section we will describe the simulated and the real signal that we will use for the demonstration of the proposed algorithm in section 3 and for quantifying the results in section 4. With the simulated recordings we can validate the sorting accuracy for all the separated neurons, while with the real recordings we can validate the accuracy only for a single neuron - the one which was simultaneously recorded with the intracellular electrode.

2.1. Simulated neural recordings

To describe the proposed algorithm in an illustrative way we will use the simulated extracellular neural recording, in order to have the precise knowledge of which neuron fired which spikes. In this way we are able to clearly demonstrate the performance of the proposed algorithm. Also, using such signal, we are able to precisely measure the sorting accuracy and the sorting detection and thus compare the proposed approach with the other approaches.

To create the recording we first generate spatial positions for 1000 artificial neurons. We distribute the neurons randomly in a 3D space, respecting some constraints about their minimal and maximal mutual distances. We place an electrode with four virtual recordings sites at four different locations around the middle of the space. Distance between two neighboring sites is set to be equal to an average distance between two neighboring neurons. To emulate the effect of extracellular medium on propagating action potentials we simulate attenuation of the amplitude, but also a moderate

waveform smoothing which arises from a lowpass filtering properties of the medium [29]. We consider the smoothing between the recording sites to be negligible and simulate only the smoothing which happens during the action potential propagation between neurons and the electrode. We assume that the action potentials fired by the same neuron are always recorded as spikes of the same shape. Moreover, since the smoothing is generally moderate, we assume that the 1000 simulated neurons exhibit only 32 different spike shapes.. The 32 shapes are in fact templates generated by averaging spikes coming from 32 different neurons, recorded by real extracellular recordings (the recordings will be described in the next subsection). The length of each template is 60 samples, corresponding to $4ms$ real time. For each neuron we first generate a random firing rate between 5Hz and 10Hz and then generate Poisson distributed firing times.

To make the simulated signal more realistic, we have to simulate the sampling effects. Indeed, in real recordings spikes coming from a particular neuron generally look different, because they are sampled at different time instants with respect to the beginning of each spike. We simulate this effect by upsampling the spike templates by a factor of 100. Then we associate the spike templates with the corresponding time locations in the signal. Finally we subsample back to the original recording rate.

Assuming an isotropic setting, the extracellular potential typically decays as $1/r^k$, where r is the Euclidian distance between the firing neuron and the recording site. Depending on the position and orientation, the power k can take the value 1 (monopole model, near the soma), 2 or higher (dipole model or multipole model, far-field). For sake of simplicity, we consider $k = 1$ in our simulation. The first column on figure 2 shows an example of the simulated recording obtained in this way. We refer to [30] and [31] for further discussions on the propagation of action potentials through the extracellular medium.

2.2. Real neural recording

A drawback of the validation using the simulated signal lies in the complexity of a real neural mixture, which is very hard to reproduce artificially. Real recordings, depending on the tissue in which the recording is taken, consist of superposed activity of up to millions of neurons. The neurons interact through the large number of dendrites and axons, what makes the spatial configuration extremely complex. Thus, the simulated signal is often not a truthful counterpart of the real signal.

Apart from the simulated signal we examine the proposed algorithm using the real neural recordings. We use the simultaneous intracellular-extracellular recordings from a rat hippocampal area CA1 done by Henze et al., and described in [11]. When the extracellular electrode is close to the intracellular, the activity of the neuron recorded intracellularly will be also visible in the extracellular recording. Of course, with the extracellular electrode activities of a vast number of neurons are recorded, so to separate the activity of individual neurons we have to do spike sorting. Figure 1 shows a part of such simultaneous recording. The four top plots show the extracellular recording

with tetrode and the bottom plot shows the corresponding intracellular recording. The action potentials fired by the neuron recorded intracellularly are clearly visible on all four extracellularly recorded channels. This indicates that the recording sites are located very close to each other.
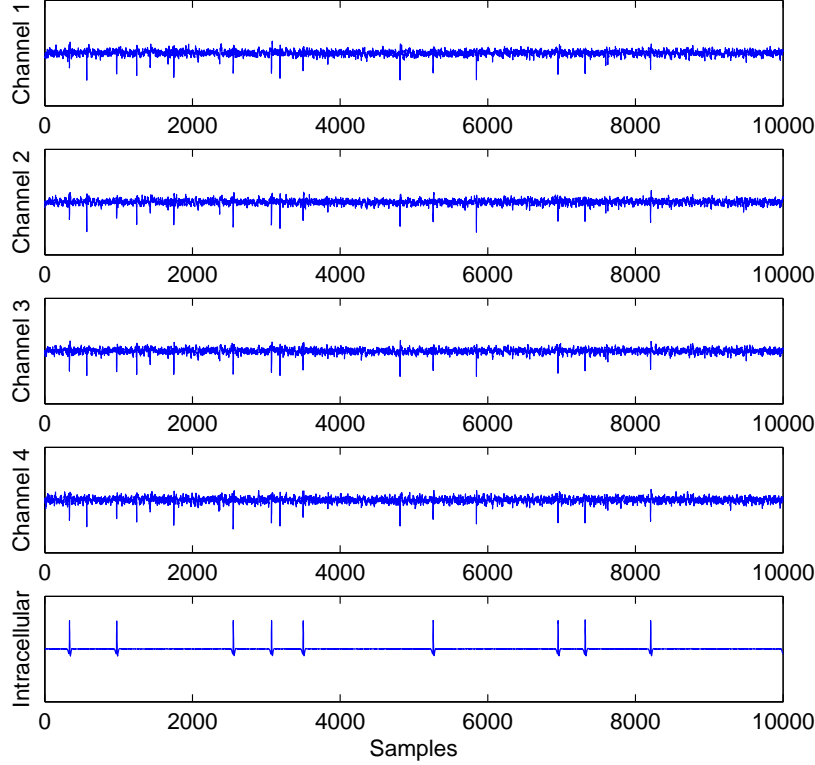

Figure 1. Simultaneous extracellular–intracellular recording. The four recording sites are very close, so the action potentials recorded with the intracellular electrode are clearly visible on all four extracellularly recorded channels.

On the plots of the extracellular channels we can also see the activity of other neurons that are around the extracellular electrode. Notice that many spikes from the other neurons have amplitudes similar to those of the spikes that come from the neuron recorded intracellularly. Thus, the task of spike sorting is obviously not trivial in this case.

3. The algorithm description

In this section we describe the proposed algorithm for multi-channel spike sorting. The algorithm iteractively removes the activities of distant neurons from the original recording as well as the activities of the neurons close to the electrode, once they are separated from the mixture. By doing so we reduce the number of sources, which brings the application of ICA in a more comfortable setting.

Apart from the recorded signal, to use the algorithm we only need to provide a lower bound for the firing rate, call it G, and the spike detection threshold level. This

lower bound is usually easy to set since, generally, we are not interested in separating the activities of neurons that fired only a few spikes. A more detailed discussion on how to chose G is given in our previous paper on spike sorting [23]. The choice of the threshold level, on the other side, is not very critical, since we will simply neglect all the spikes that belong to the cluster which has the lowest average peak-to-peak amplitude of the spikes. This will make the algorithm more reliable, since the spikes with the lowest amplitudes usually come from many different neurons, whose activity is only partially detected.

We assume that a four-channel recording is given, but the algorithm is the same for any number of channels. The four recorded signals are labeled as $E1$, $E2$, $E3$ and $E4$. An example of a part of the simulated four-channel recording is shown on figure 2 and of the four-channel real recording on figure 3. Spikes from the neuron recorded intracellularly are marked with the red stars.
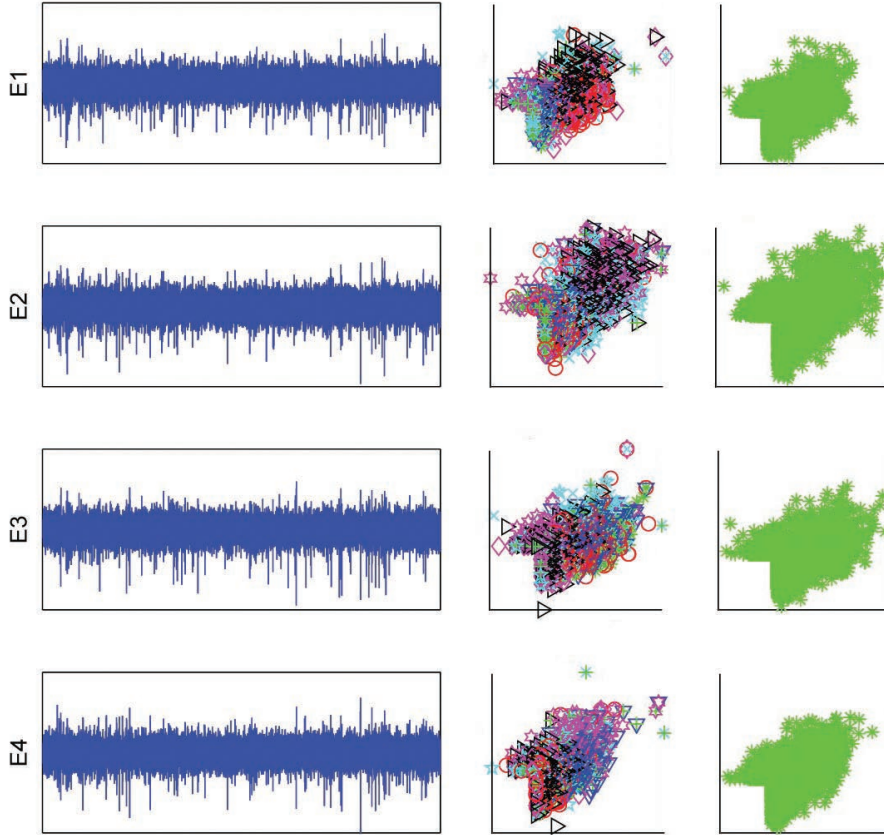

Figure 2. 5000 samples from the simulated four-channel extracellular recording (first column). 2D feature vector space with the extracted spikes - positive peak amplitude vs negative peak amplitude (second column). Results of sorting algorithm from [23] are given in the third column (only one cluster was detected for each channel).

To demonstrate that spike sorting is very difficult for such recording we apply directly the greedy based spike sorting method described in [23]. First, we detect the spikes using the spike detection method described in [9] and [32]. We then project
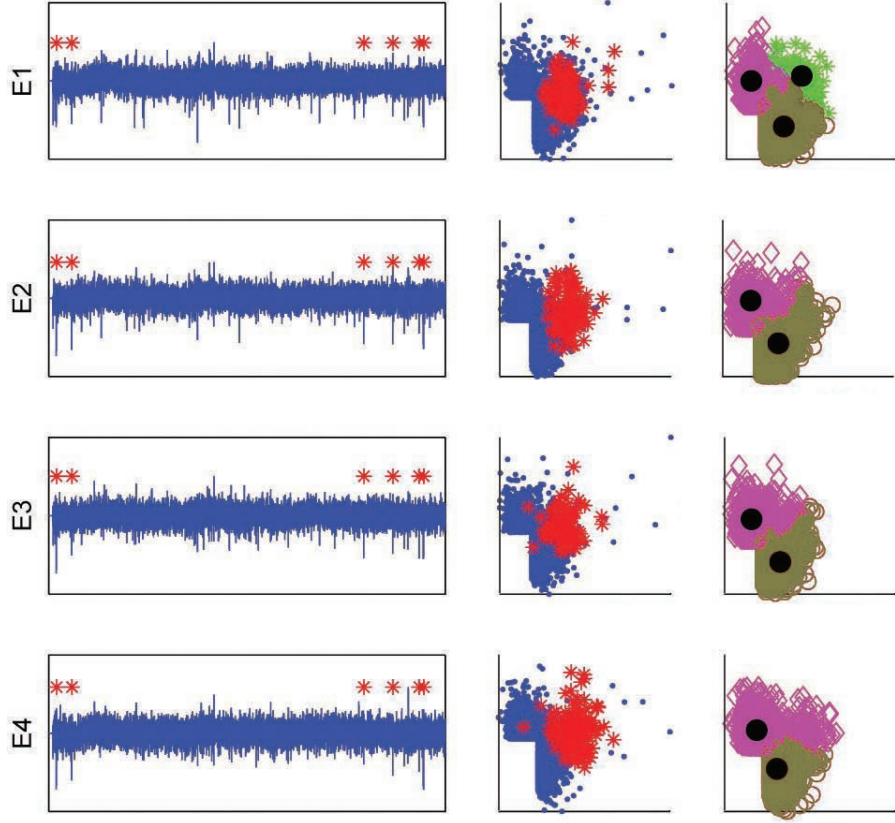
Figure 3. 5000 samples from the real four-channel extracellular recording (first column). 2D feature vector space with the extracted spikes - positive peak amplitude vs negative peak amplitude (second column). Spikes that come from the neuron recorded intracellularly are labeled with the red stars, while the rest of the spikes are labeled with the blue dots. Results of sorting algorithm from [23] are given in the third column, where the black dots marks are the detected centers of the clusters.

the spikes in a 2D vector space by keeping only two features per spike: the positive and the negative peak amplitudes. Notice that one could also use, e.g., the two first principal components. In the particular case, better (generally more reliable) results were obtained when the positive and the negative peak amplitude were used as the features, instead of the commonly applied PCA. The plots of the features are shown next to the corresponding signals, in the second column on figures 2 and 3. In the third column on figures 2 and 3 we give the outputs of the algorithm from [23]. The spikes that are left unsorted by the algorithm are automatically eliminated and not plotted. Note that the colors/symbols chosen for the representation of the clusters for the plots in the second column are not related to the one in the third column. It is evident that from such feature vector space it is not possible to do an accurate spike sorting.

We will now demonstrate the performance of the proposed algorithm using step-by-step description. The flowchart that describes the proposed algorithm is shown on figure 4.

- `Step 1:` **ICA.** We process the input signal with the FastICA algorithm described
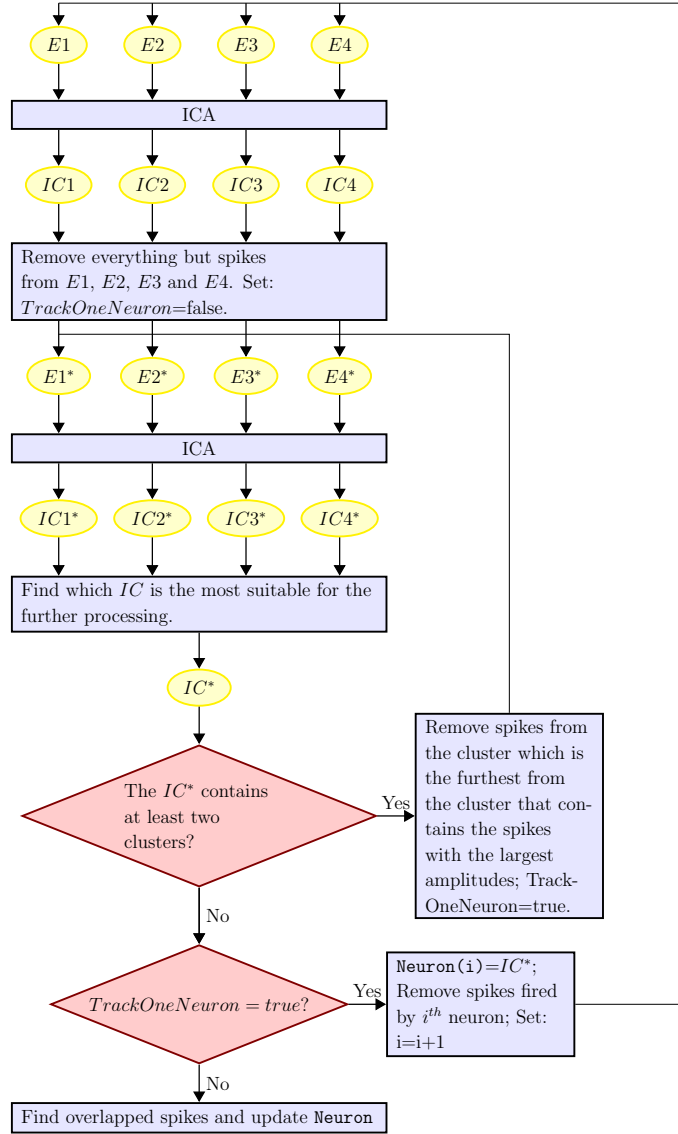
Figure 4. Flowchart of the proposed multi-channel spike sorting algorithm.

in [28] (we used the default parameters given within the FastICA MATLAB package) and obtain $IC1$, $IC2$, $IC3$ and $IC4$ as the outputs (figures 5 and 6). The second and the third column on the both figures are again shown only to give an illustration of what the results would be if the feature extraction based sorting method was directly applied on the outputs of the ICA algorithm. The difference between the clusters is more obvious than on figures 2 and 3.

• Step 2: **Remove everything but spikes from $E1$, $E2$, $E3$ and $E4$. Set: k=false.** We first want to find which one of the four ICs contains the largest projection of the spikes from neurons close to the electrode. The criterion we set to determine this IC is spike dynamics. As a measure of the spike dynamics we use the average difference between the positive and the negative peak. Since spikes naturally contain a large peak, such difference should be a good measure of the dynamics. We first find
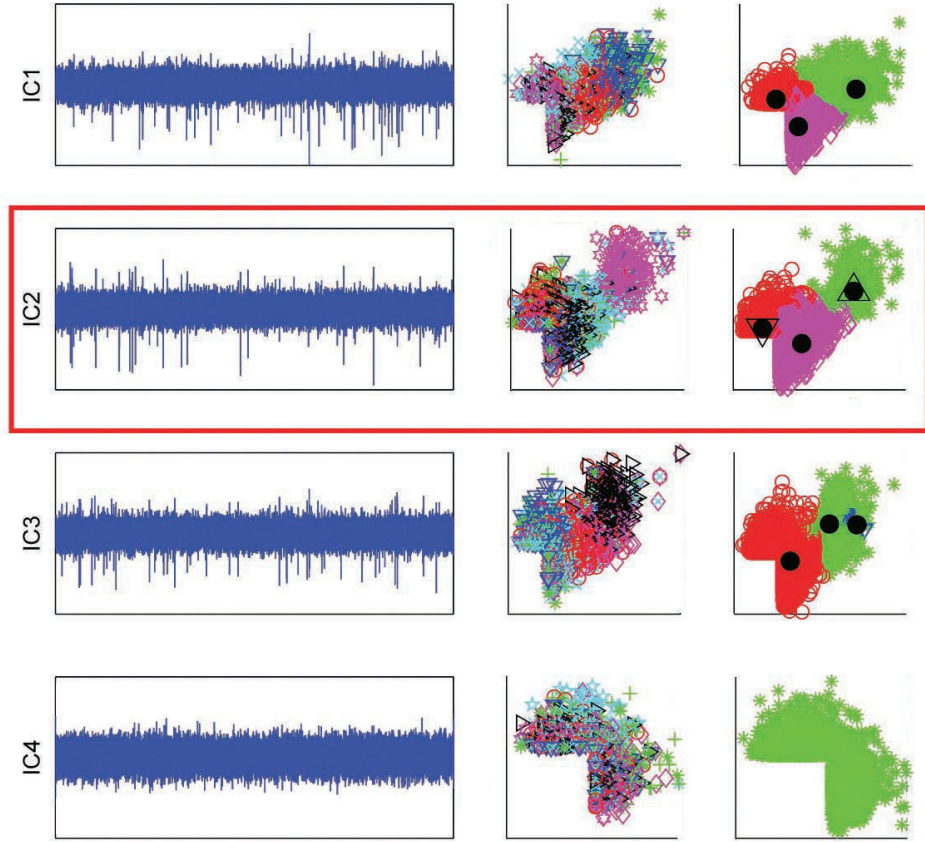
Figure 5. Result of applying ICA on the recording shown on figure 2. The four *IC*s are shown in the first column (5000 samples). 2D feature vector space with the spikes extracted from the *IC*s are in the second column. The plots in the third column display the results of applying the algorithm from [23] on the vector space from the second column. The red rectangle marks the IC that has the largest spike dynamics.

all the spikes from all four *IC* using the method described in [9] and [32]. Then, we calculate the corresponding spike dynamics for each *IC* and consider as actual spikes only those detected from the IC with the largest spike dynamics. Next, from all the 4 input recordings we remove (set to zero) all but the actual spikes. We assume that the removed parts of the signal correspond only to the noise and the cumulative activity of the neurons that are distant from the electrode. The outputs are called $E1^*$, $E2^*$, $E3^*$ and $E4^*$.

    • Step 3: **ICA.** We apply ICA on $E1^*$, $E2^*$, $E3^*$ and $E4^*$. The resulting *IC*s, called $IC1^*$, $IC2^*$, $IC3^*$ and $IC4^*$, are shown on figure 7 for the simulated signal and on figure 8 for the real signal. To demonstrate the results as before, we plot the spikes in the feature vector space (second column) and output of the greedy sorting algorithm from [23] (third column). As the number of the sources is now lower, the ICA algorithm performed a little better and a little bigger difference between the clusters is visible, in comparison with the results from figures 5 and 6.
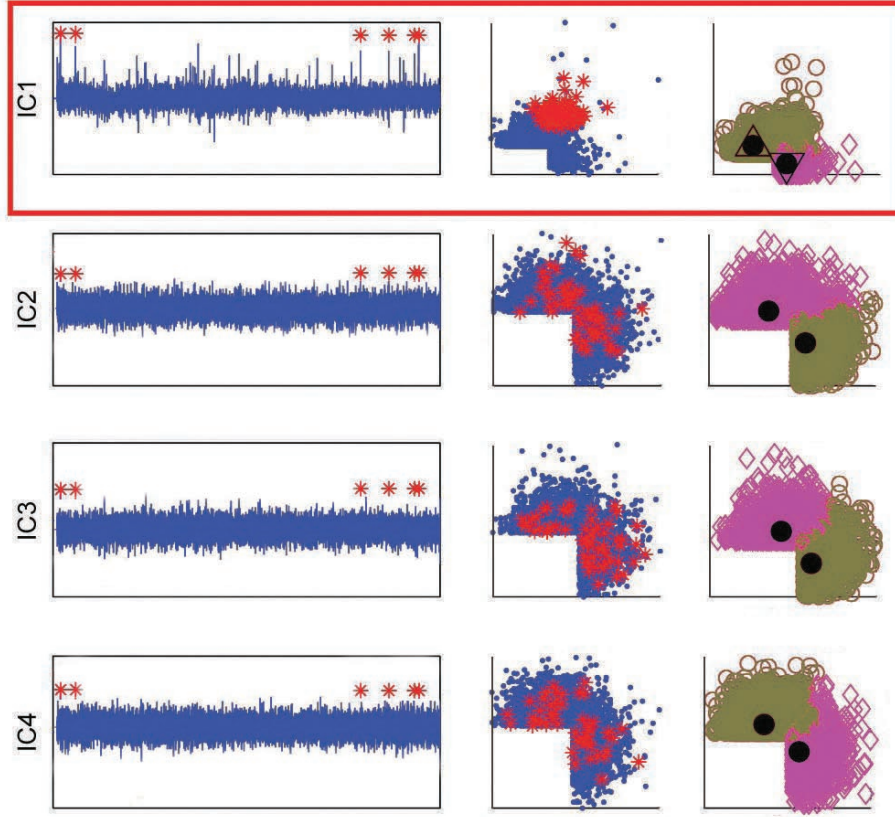
Figure 6. Result of applying ICA on the recording shown on figure 3. The four *IC*s are shown in the first column (5000 samples). 2D feature vector space with the spikes extracted from the *IC*s are in the second column. The plots in the third column display the results of applying the algorithm from [23] on the vector space from the second column. The red rectangle marks the IC that has the largest spike dynamics.

- `Step 4:` **Find which *IC* is the most suitable for the further processing.** In the further steps we will need only one *IC*. Thus in this step we want to chose the one which contains well preserved spike waveforms. It is likely that a good choice would be the one for which the detected spikes have the largest dynamics. We calculate the spike dynamics in the same way as in the `step` 2. For the further processing we chose the *IC* which has the largest value of the dynamics and call it IC^*.
- `Condition 1:` **The IC^* contains at least two clusters?**
- `If` `Condition 1` `is` true: **Remove spikes from the cluster which is the furthest from the cluster that contains the spikes with the largest amplitudes; TrackOneNeuron=true.** In this step we have to apply the spike sorting algorithm proposed in [23], this time it is not only for demonstration, but to find which spikes we can remove from the signal. For each cluster we compute the spike dynamics as the average of peak-to-peak amplitudes from the first G spikes. The spikes that have been classified in the cluster furthest from the one with the largest spike dynamics are now removed from $E1^*$, $E2^*$, $E3^*$ and $E4^*$. Next, the algorithm goes back to `step`
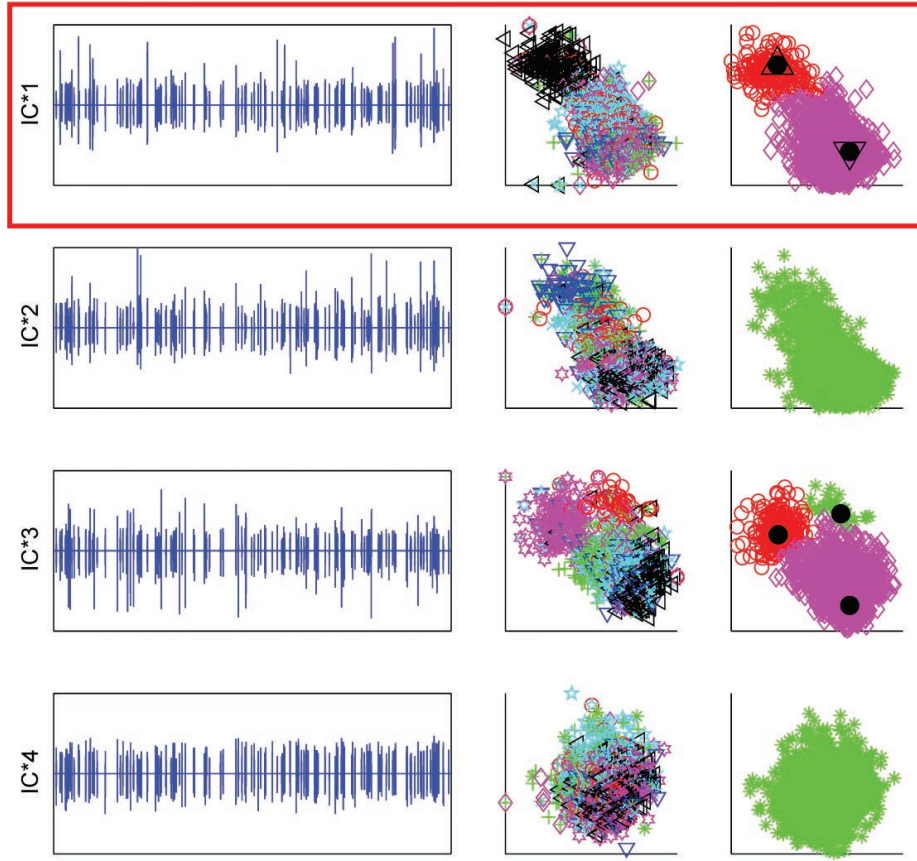
Figure 7. Result of applying ICA on the simulated recording after all but spikes was removed from the signal (set to zero) - 5000 samples are displayed. The four *IC*s are shown in the first column. 2D feature vector spaces with the spikes extracted from the *IC*s are in the second column. The plots in the third column display the results of applying the algorithm from [23] on the vector space from the second column. IC that has been chosen for the further processing is marked with a red rectangle. The black triangle, with the tip pointing up, marks the center of the cluster that contains the spikes with the largest dynamics. Opposite, the black triangle with the tip pointing down marks the center of the cluster that contains the spikes with the smallest dynamics.

3. We show on figures 9 and 10 the outputs after applying ICA on the new $E1^*$, $E2^*$, $E3^*$ and $E4^*$ for the simulated and the real recording respectively. From the simulated recording (figure 9) we have detected only one cluster on each of four *IC*. We use the same criterion as before to chose which *IC* we should keep. Since the *condition 1* is now `false`, the algorithm will continue to the *condition 2*. Notice that almost all the remaining spikes are fired by the same neuron. From the real recording (figure 10) we have detected more than one cluster on $IC1^*$ and $IC2^*$; for the further processing we will use $IC1^*$. The cluster that will be removed is the one labeled with a black triangle whose tip is pointing down. After that cluster is removed, spikes from the neuron recorded intracellularly will be almost the only one remaining in the signal. Only a
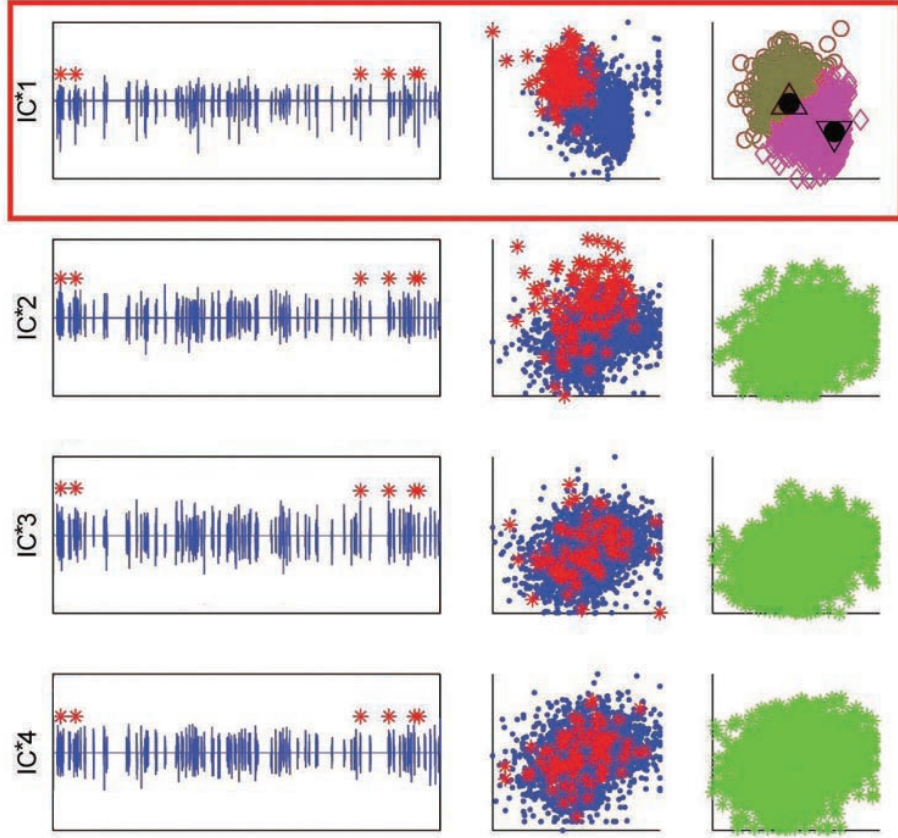
Figure 8. Result of applying ICA on the real recording after all but spikes was removed from the signal (set to zero) - 5000 samples are displayed. The four *IC*s are shown in the first column. 2D feature vector spaces with the spikes extracted from the *IC*s are in the second column. The plots in the third column display the results of applying the algorithm from [23] on the vector space from the second column. All the labels are the same as for figure 7.

few spikes from the intracellularly recorded neuron were removed. We set in this step the flag *TrackOneNeuron*, in order to track if the algorithm converged just after a new neuron is separated, what would indicate generally that no more neurons can be separated from the given recording.

• If *Condition 1* is false: *Condition 2:*   **TrackOneNeuron = true?**

• If *Condition 2* is true: **Neuron(i)=IC^*; Remove the spikes fired by the ith neuron; Set:** $i = i + 1$. If *TrackOneNeuron* is true that means that we have detected more than one cluster in the previous iteration so now, since only one cluster is left (the *condition 1* was false), we assume that the remaining spikes are coming from the same neuron. This is the ith separated neuron. To continue our iterative algorithm we set to zero all the samples from the recording (from $E1$, $E2$, $E3$ and $E4$) when any of the already detected neurons (Neuron(1), Neuron(2),...,Neuron(i)) was active and go back to **step 1**. By doing this we removed an important high amplitude sources.

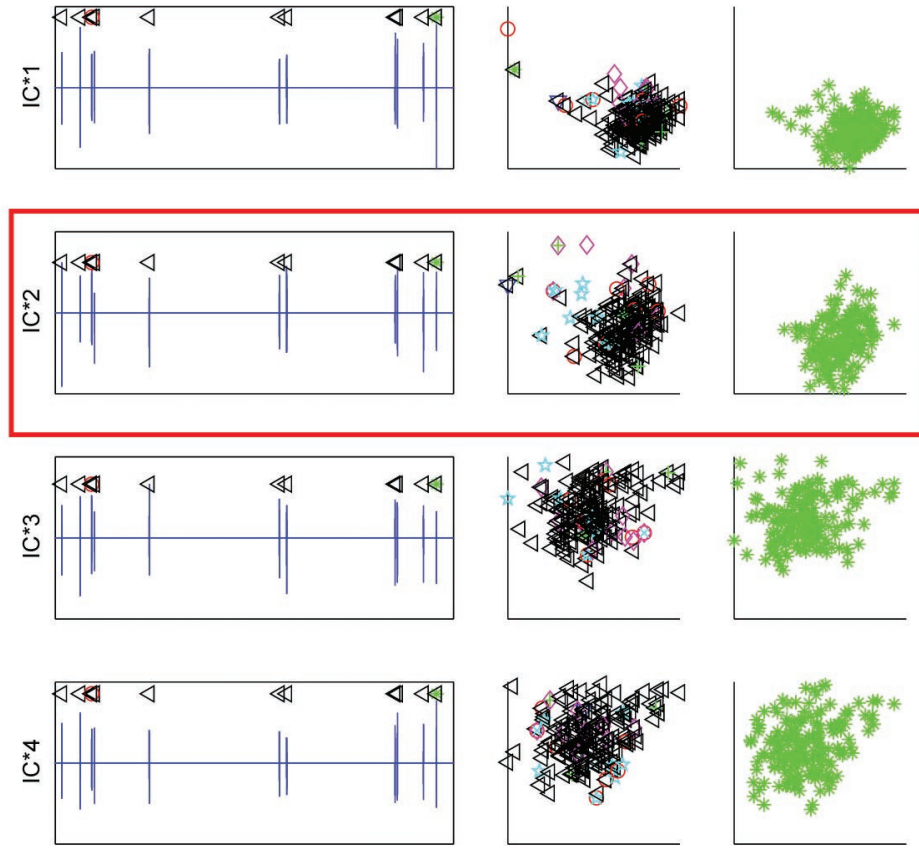• If *Condition 2* is false: **Find the overlapped spikes and update**

Figure 9. Result of applying ICA on the simulated recording, after removing (setting to zero) of the low amplitude spikes (see figure 7) from $E1^*$, $E2^*$, $E3^*$ and $E4^*$ (5000 samples). The four *IC*s are shown in the first column. 2D feature vector spaces with the spikes extracted from the *IC*s are in the second column. The plots in the third column display the results of applying the algorithm from [23] on the vector spaces from the second column. All the labels are the same as for figure 7.

`Neuron`. This is the last step of the proposed algorithm. We address now a very important problem in spike sorting: simultaneous firing. The proposed deflation based algorithm is obviously not able to detect simultaneous firing, since once a spike has been sorted the corresponding part of the signal is set to zero for the following iterations. Thus, if two or more neurons fired at approximately the same time, the spike will be assigned only to one of these neurons. To find the simultaneously fired spikes we analyze the activity of the sorted neurons two by two, for all possible pairs of the detected neurons. When analyzing the activity of each pair, we keep in the recording only the segments when one of the neurons in the pair fired a spike. Each such recording, call it
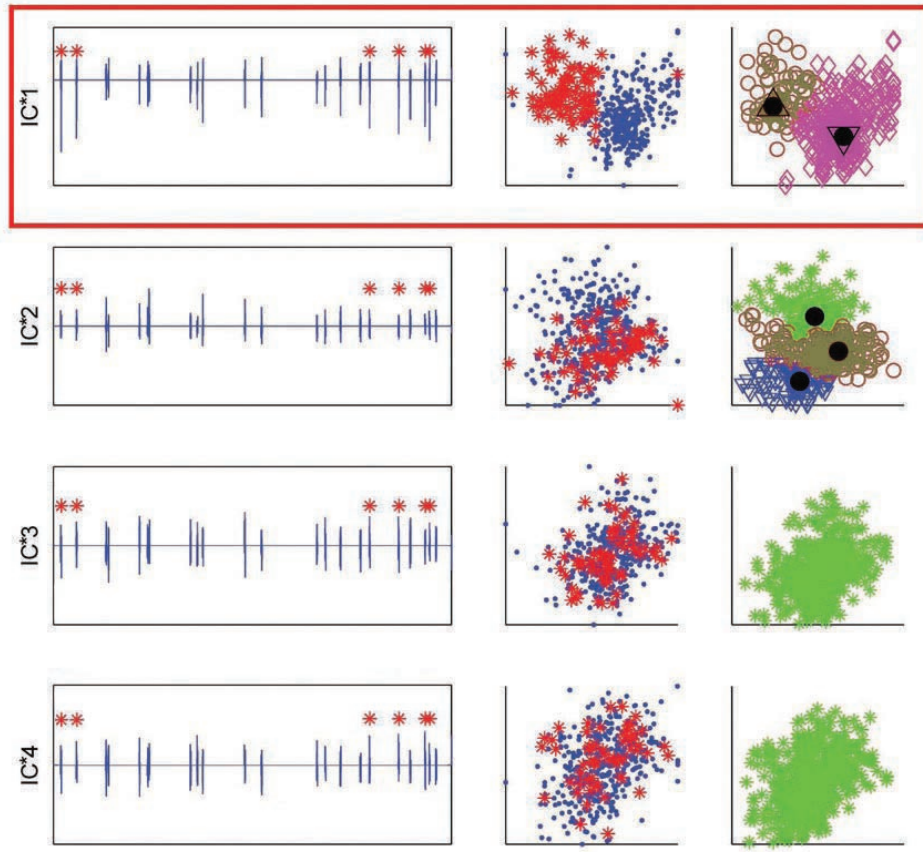
Figure 10. Result of applying ICA on the real recording, after removing (setting to zero) of the low amplitude spikes (see figure 8) from $E1^*$, $E2^*$, $E3^*$ and $E4^*$ (5000 samples). The four ICs are shown in the first column. 2D feature vector spaces with the spikes extracted from the ICs are in the second column. The plots in the third column display the results of applying the algorithm from [23] on the vector spaces from the second column. All the labels are the same as for figure 7.

$\tilde{s}_{i,j}$, where $i = 1, ..., S - 1$ and $j = i + 1, ..., S$ can be expressed‡ as:

$$\tilde{s}_{i,j} = s_i + s_j + (1 - \delta(|s_i| + |s_j|)) \sum_{k=1, k \neq i,j}^{S} s_k,$$

where S is the number of sorted neurons and where $\delta(u)$ takes the value 1 for $u = 0$ and 0 elsewhere. Notice that we use absolute values of s_i and s_j to exclude the pairs i, j such that $s_i = -s_j \neq 0$. It is obvious that most of the energy in any $\tilde{s}_{i,j}$ comes from s_i and s_j. Thus, applying ICA on $\tilde{s}_{i,j}$ leads to the separation of s_i and s_j: one IC will represent mostly s_i, another one s_j and the remaining ICs will represent $(1 - \delta(|s_i| + |s_j|)) \sum_{k=1, k \neq i,j}^{S} s_k$. Since the activity of s_i and s_j will be separated, any

‡ For notational simplicity, we drop the time argument and write s_k instead of $s_k(t)$ for the recorded activity of neuron #k. Note that $s_k(t)$ is a sparse signal: We have $s_k(t) = 0$ except for intervals $[\tau, \tau + T]$ when an action potential is emitted from time τ. The length T of the interval corresponds to the duration of an action potential.

spikes fired simultaneously by these two neurons should be visible on both of the *IC*s that represent the activity of these neurons. We demonstrate this by an example shown in figure 11. In the first two rows we plot part of the activity of two simulated neurons that fired three spikes simultaneously. The next four plots show four channels of the simulated recording. The activity of the two neurons is visible, but hard to recognize, especially to separate. We remove from the four channels everything but the segments when any of the two neurons was active and apply ICA on such sparse signal. The result of ICA is shown on four bottom plots on the same figure. Since this is the last step of the proposed algorithm, we already have the estimation of the activity of all the separated neurons. Thus, it is easy to find, from the result of ICA, that in this example $IC2$ represents the activity of *Neuron 1* and that $IC3$ represents the activity of *Neuron 2*. All the overlapped spikes are visible on both $IC2$ and $IC3$. They are now very easy to localize and to update the detected activity of the separated neurons.

4. Results

We apply the algorithm described in the previous section on 5 real recordings and on 10 simulated recordings. The results are given in tables 1 and 2. There are four key-operations in the proposed algorithm: 1) removing of the noise (*Noise rem.*); 2) removing of the spikes from the clusters far from the one that contains the spikes which show the largest average peak-to-peak amplitude (*Clus. rem.*); 3) removing of the spikes from already separated neurons (*Sorted rem*); 4) detection of the overlapped spikes (*Over. det.*). We analyze contribution of each of these steps by simply comparing the proposed algorithm to the algorithms which perform none, only one or more of these steps. Namely, we compare the proposed algorithm with the following:

 (i) Only the spike sorting algorithm, without performing ICA (*Spike sor.*).
 (ii) ICA and spike sorting
(iii) ICA, spike sorting and removal of the spikes from already separated neurons.
(iv) As 3, but with removal of everything but spikes (`step 2` of the algorithm).
 (v) As 4, but with removal of clusters that generally contain spikes small in the amplitude (clusters which are far from the one that contains the spikes which show the largest average peak-to-peak amplitude).

The proposed algorithm is actually an extension of the algorithm (v), with a sequence for the detection of the overlapped spikes.

We express the results through two parameters: 1) sorting accuracy ($SA(\%)$) which we define as ratio of accurately sorted spikes and total number of detected spikes and 2) sorting detection ($SD(\%)$) which we define as ratio of accurately sorted spikes and total number of spikes in the signal.
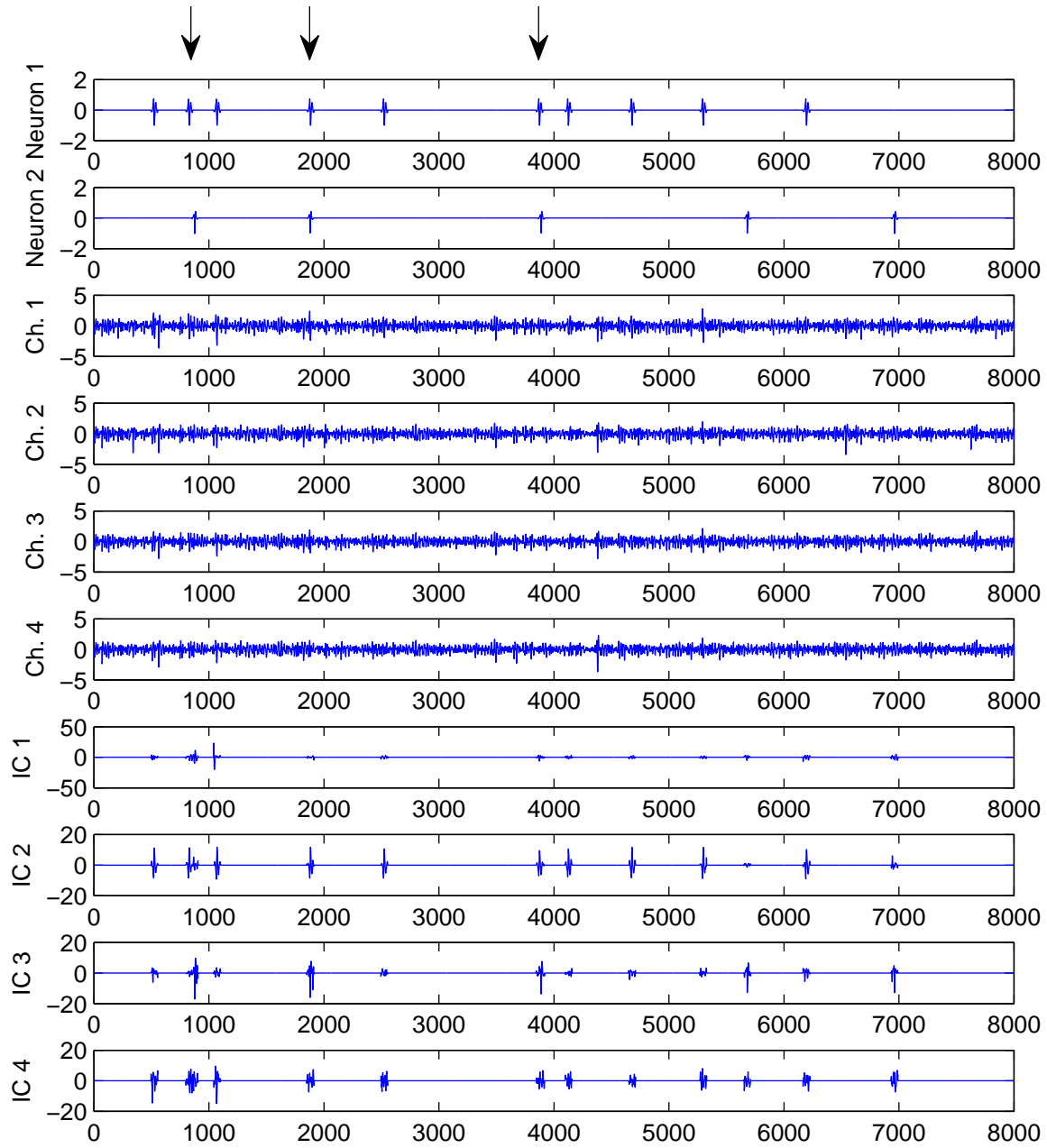
Figure 11. The first two plots show part of the activity of the two simulated neurons. The following four plots show the part of the four-channel simulated recording. The four plots at the bottom show the results of applying ICA on the four channels. Before applying ICA the recording was modified by setting to zero all but the segments where one of the two neurons was active. It appears that the activity of *Neuron 1* is represented by *IC3* and the activity of *Neuron 2* is represented by *IC1*. The three arrows on the top of the figure point out the overlapped spikes from the two neurons. All of the three overlapped spikes are successfully sorted.

4.1. Results of the spike sorting on the real signal

For the real recordings we can quantify the results only for one neuron per recording, the one which was simultaneously recorded intracellularly. Thus SA and SD are very

Table 1. Comparison of different spike sorting algorithms for 5 real recordings, in terms of sorting accuracy (SA) and sorting detection (SD).

Recording	Spike sorting		Spike sorting ICA		Spike sorting ICA Sorted rem.		Spike sorting ICA Sorted rem. Noise rem.		Spike sorting ICA Sorted rem. Noise rem. Clus. rem.		Spike sorting ICA Sorted rem. Noise rem. Clus. rem. Over. det.	
	SA %	SD %	SA %	SD %	SA %	SD %	SA %	SD %	SA %	SD %	SA %	SD %
d561102	79	64	83	93	83	93	90	92	93	92	93	92
d561103	32	97	48	95	52	85	83	83	89	80	89	86
d561104	21	98	33	96	49	88	75	87	83	84	84	89
d533101	73	33	64	74	64	74	78	72	80	73	80	73
d533102	64	48	80	87	80	87	88	85	92	82	92	83

simple to calculate: $SA(\%) = 100 * C/(F + C)$ and $SD(\%) = 100 * C/T$. Here C is the largest number of the spikes from the neuron recorded intracellularly, which are sorted into the same cluster (correct detections). F is the number of spikes from other neurons which are wrongly placed into the same cluster for which C is calculated (false spikes). T is the total number of spikes fired by the intracellularly recorded neuron.

In table 1 and on figure 12 we give SA and SD for each of the real recordings. Names of the recordings are kept from [11]. Durations of the recordings were from 60 to 120 seconds with the sampling frequency of 10kHz for some recordings and 20kHz for others. The total number of the detected spikes per recording was from 800 to 2000, while the number of the spikes fired by the intracellularly recorded neuron was from 200 to 500.

The results suggest that the proposed approach improves significantly the sorting results in comparison with the basic spike sorting algorithm and the ICA algorithm. It generally decreases the number of falsely sorted spikes and increases the number of spikes that are left unsorted (missed spikes). As we mentioned in the introduction, in the trade-off between the number of missed spikes and the number of false spikes it is generally highly preferable to have more missed spikes.

When the intracellularly recorded neuron is sorted first (recordings d561102, d533101 and d533102) there is no benefit from the removal of the spikes from already sorted neurons (results in the third and the fourth column of table 1 are the same in such cases). Also, for those recordings contribution from detection of the overlapped spikes is very small, since most of the overlapped spikes were initially correctly assigned to the intracellularly recorded neuron (results in the last two columns of table 1 are the same/similar in such cases).

4.2. Results of the spike sorting on the simulated signal

Using simulated recordings we can quantify the results for more than one neuron and also we can easily perform several simulations and average their results. For each
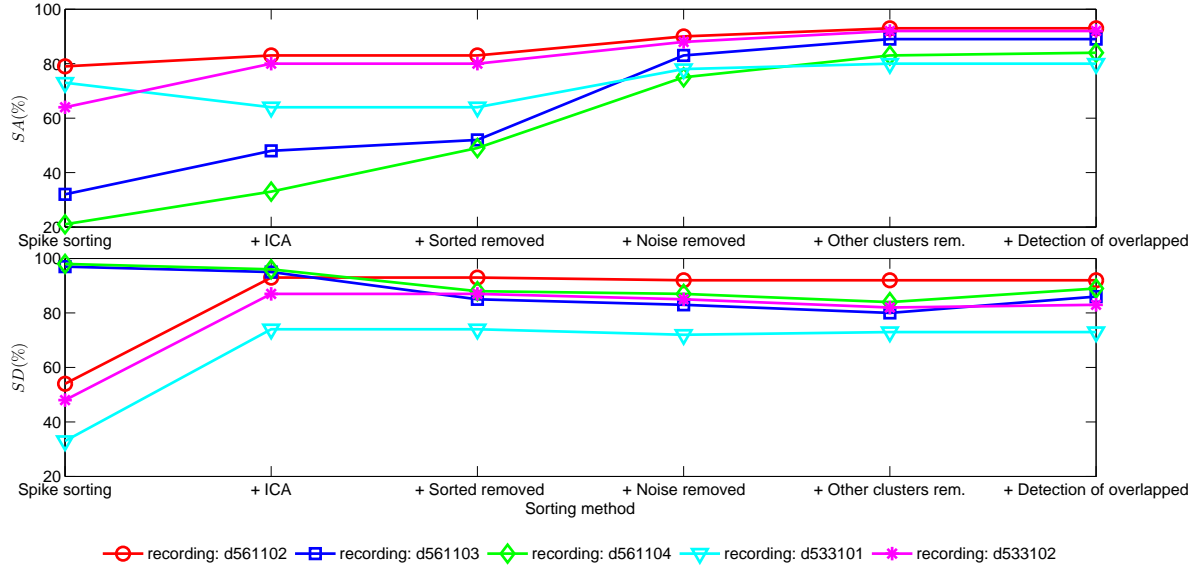
Figure 12. Comparison of different spike sorting algorithms for 5 real recordings, in terms of sorting accuracy (SA) and sorting detection (SD).

simulated recording we set the maximum number of outer loops (sorted neurons) to 6. However, in some situations (especially for simpler methods like the basic spike sorting and combination of the basic spike sorting with ICA) less than 6 neurons have been found.

Here we do a computation of SA and SD in a slightly different way than for the real signal. We compute the average $\bar{SA}$ and the average $\bar{SD}$ over 10 simulations for each jth sorted neuron, where j goes from 1 to 6, which is the maximum number of the sorted neurons:

$$\bar{SA}_j = \frac{\sum_{i=1}^{N_j} SA_{i,j}}{N_j}, \bar{SD}_j = \frac{\sum_{i=1}^{N_j} SD_{i,j}}{N_j}$$

where N_j is the number of iterations in which at least j neurons were detected. We give also a standard deviation (sd) of $\bar{SA}$ and $\bar{SD}$ in order to quantify the robustness of each algorithm.

The results are given in table 2 and on figure 13. Even though the results vary significantly from neuron to neuron (spikes from the neurons close to the electrode are, as expected, sorted much more accurately that from the more distant ones), we can say again that overall each step of the proposed algorithm leads to significant improvement of the final results.

An important property of the proposed algorithm is that increasing SA is paid by decreasing SD as well, as is even more evident than on the figure 12. However, the last step (detection of overlapped spikes) increases SD, especially as j increases, since for the larger j (more distant neurons) many spikes were not detected because they overlapped spikes from the closer neurons (which correspond to the lower j).

The standard deviation is larger for the neurons further from the electrode and tends to decrease as a more complex algorithm is used. The standard deviation illustrates the

Table 2. Comparison of different spike sorting algorithms in terms of average sorting accuracy ($\bar{SA}$), average sorting detection ($\bar{SD}$) and their standard deviations (sd) for the first 6 sorted neurons.

j	Spike sorting					Spike sorting ICA					Spike sorting ICA Sorted rem.					Spike sorting ICA Sorted rem. Noise rem.					Spike sorting ICA Sorted rem. Noise rem. Clus. rem.					Spike sorting ICA Sorted rem. Noise rem. Clus. rem. Over. det.				
	$\bar{SA}$ %	sd	$\bar{SD}$ %	sd	N	$\bar{SA}$ %	sd	$\bar{SD}$ %	sd	N	$\bar{SA}$ %	sd	$\bar{SD}$ %	sd	N	$\bar{SA}$ %	sd	$\bar{SD}$ %	sd	N	$\bar{SA}$ %	sd	$\bar{SD}$ %	sd	N	$\bar{SA}$ %	sd	$\bar{SD}$ %	sd	N
1	18	15	97	5	10	68	12	93	9	10	76	10	91	7	10	85	8	90	7	10	88	6	87	6	10	88	6	88	6	10
2	45	7	80	7	2	62	13	90	10	10	74	11	86	8	10	84	8	84	7	10	86	7	81	6	10	86	7	84	6	10
3	0	0	0	0	0	54	14	85	18	5	69	13	79	11	10	78	9	78	10	10	81	7	75	8	10	82	7	80	8	10
4	0	0	0	0	0	44	16	82	12	2	60	15	77	12	10	72	11	76	12	10	78	9	72	11	10	79	9	76	10	10
5	0	0	0	0	0	0	0	0	0	0	54	16	74	16	9	68	14	72	15	10	74	11	71	11	10	75	11	74	11	10
6	0	0	0	0	0	0	0	0	0	0	39	17	70	18	7	65	15	67	17	9	72	11	66	12	9	73	11	70	12	9

stability of the results, e.g., for distant neurons sometimes the sorting results are good, but sometimes they are quite bad, indicated by larger standard deviation. On the other hand results for neurons very close to the electrode are always relatively good, thus the standard deviation of the results is lower.
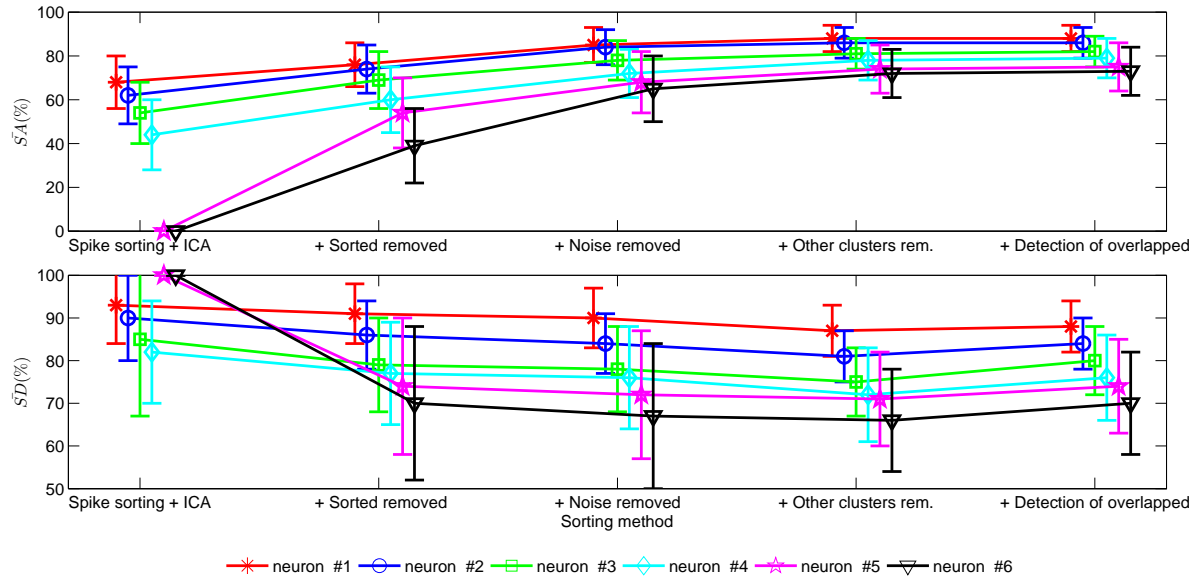

Figure 13. Comparison of different spike sorting algorithms in terms of average sorting accuracy ($\bar{SA}$) and average sorting detection ($\bar{SD}$) for the first 6 sorted neurons. The length of the perpendicular lines corresponds with the standard deviation of $\bar{SA}$ or $\bar{SD}$ for the particular algorithm and the particular neuron. The neurons are labeled with respect to their minimum distance to the electrodes.

5. Discussion

In this paper we proposed a new algorithm for spike sorting from multi-channel recordings. We use iterative application of ICA and deflation to sort the spikes. Activity at the recording sites is mutually highly dependant, while the activity of single neurons is mutually much less dependant. This naturally suggests application of ICA to separate the neural mixture.

A condition that the number of sensors should be equal or greater than the number of sources appears as the major problem and limitation for application of ICA on neural recordings. The proposed algorithm uses deflation to eliminate or at least to reduce the contribution of different sources. In particular, we remove: 1) everything but spikes, 2) spikes which have already been sorted and 3) spikes which belong to the clusters far from the one which contains the spikes of the largest average peak-to-peak amplitude.

Such deflation would result in inability of the algorithm to detect spikes fired by different neurons at approximately the same time - simultaneous firing. Only one spike per simultaneous firing could be detected. The solution to this problem is implemented as the last step of the proposed algorithm. We take two of the separated neurons and keep in the recording only the segments in which one of these two neurons was active. Then we apply ICA on such sparse signal. Since we have only two high-energy sources in the signal, ICA will, in most situations, be able to separate the activity of the two neurons, including simultaneously fired spikes. We repeat this procedure for all the possible pairs of the separated neurons.

The results given in tables 1 and 2 suggest that each step of the algorithm improves the final sorting results. Overall, the algorithm significantly increases the number of correctly sorted spikes while increasing the number of missed spikes by a relatively small amount. ICA alone was not sufficient to obtain reliable results. It is important to mention that if a recording is very noisy, the proposed algorithm will not be able to detect any cluster.

In some particular cases, such as multi-electrode recordings from peripheral nerve interfaces, the spike waveforms can arrive to the different recording sites with time delays up to 0.1ms [33], [34]. FastICA algorithm is not adapted for such mixtures. In its present form, the proposed algorithm is therefore not suitable for those cases. Nonetheless, the proposed deflation methodology would still be useful if FastICA is replaced by some convolutive version of ICA. In the convolutive case [35], [36], the recorded mixture is described by an FIR filter model of the mixing process. Such model could be beneficial in this particular case of spike sorting for two reasons: 1) Ability to account for different delays of the source components; 2) Ability to account for echoes coming from different parts of a nerve around the electrode.

As spike features we used simply positive and negative peak amplitude. However, we could use practically any feature extraction method. Methods that can make the difference between the spikes fired by different neurons more evident will of course lead to better performance of the proposed algorithm, in terms of the number of sorted

neurons and the sorting accuracy. Nevertheless, no matter how good the chosen feature extraction technique is, the proposed algorithm should always improve the final sorting results when they are compared to the results obtained with only ICA algorithm. Finally we can say that the obtained results suggest that the proposed algorithm gives better sorting results as compared to ICA.

Acknowledgments

References

[1] J. D. Simeral, S. P Kim, M. J. Black, J. P. Donoghue, and L. R. Hochberg. Neural control of cursor trajectory and click by a human with tetraplegia 1000 days after implant of an intracortical microelectrode array. *Journal of Neural Engineering*, 8(2), April 2011.

[2] *Cerebus Data Acquisition System - users manual*. Blackrock Microsystems, 2009.

[3] M. S. Lewicki. A review of methods for spike sorting: the detection and classification of neural action potentials. *Network (Bristol, England)*, 9(4):53–78, November 1998.

[4] S. Gibson, J. W. Judy, and D. Markovic. Comparison of spike-sorting algorithms for future hardware implementation. *Annual Internationa Conference of the IEEE Engineering in Medicine and Biology Society*, 1:5015–20, 2008.

[5] E. N. Brown, R. E. Kass, and P. P. Mitra. Multiple neural spike train data analysis: state-of-the-art and future challenges. *Nature neuroscience*, 7(5):456–461, May 2004.

[6] C. Pouzat, O. Mazor, and G. Laurent. Using noise signature to optimize spike-sorting and to assess neuronal classification quality. *Journal of Neuroscience Methods*, 122(1):43–57, Dec 2002.

[7] K. H. Kim and S. J. Kim. Neural Spike Sorting Under Nearly 0-dB Signal-to-Noise Ratio Using Nonlinear Energy Operator and Artificial Neural-Network Classifier. *IEEE Transactions on Biomedical Engineering*, 47(10):1406–1411, Oct 2000.

[8] Z. Nenadic and J. W. Burdick. Spike detection using the continious wavelet transform. *IEEE Transactions in Biomededical Engineering*, 52:74–87, 2005.

[9] Z. Tiganj and M. Mboup. Spike detection and sorting: Combining algebraic differentiations with ica. In *Independent Component Analysis and Signal Separation, 8th International Conference*, pages 475–482, Paraty, Brazil, 2009.

[10] N. G. Ilan and H. J. Don. Information theoretic bounds on neural prosthesis effectiveness: The importance of spike sorting. In *ICASSP*, pages 5204–5207, 2008.

[11] D. A. Henze, Z. Borhegyi, J. Csicsvari, A. Mamiya, K. D. Harris, and G. Buzsaki. Intracellular features predicted by extracellular recordings in the hippocampus in vivo. *Journal of Neurophysiology*, 84(1):390–400, July 2000.

[12] D. A. Adamos, E. K. Kosmidis, and G. Theophilidis. Performance evaluation of PCA-based spike sorting algorithms. *Computer Methods and Programs in Biomedicine*, 91:232–244, September 2008.

[13] R. Q. Quiroga, Z. Nadasdy, and Y. B. Shaul. Unsupervised spike detection and sorting with wavelets and superparamagnetic clustering. *Neural Computing*, 16(8):1661–1687, August 2004.

[14] E. Hulata, R. Segev, and E. Ben-Jacob. A method for spike sorting and detection based on wavelet packets and Shannon's mutual information. *Journal of neuroscience methods*, 117(1):1–12, May 2002.

[15] Y. Ghanbari, L. Spence, and P. Papamichalis. A graph-Laplacian-based feature extraction algorithm for neural spike sorting. In *31st Annual International Conference of the IEEE*

Engineering in Medicine and Biology Society, 3-6 Sept. 2009, pages 3142–5, Piscataway, NJ, USA, 2009.

[16] E. Chah, V. Hok, A. Della-Chiesa, J. J. H. Miller, S. M. O'Mara, and R. B. Reilly. Automated spike sorting algorithm based on Laplacian eigenmaps and k-means clustering. *Journal of neural engineering*, 8(1), February 2011.

[17] S. Takahashi, Y. Anzai, and Y. Sakurai. A new approach to spike sorting for multi-neuronal activities recorded with a tetrode–how ICA can be practical. *Neuroscience research*, 46(3):265–272, July 2003.

[18] F. Wood, M. Fellows, J. Donoghue, and M. Black. Automatic spike sorting for neural decoding. In *Proceedings of the 26th Annual International Conference of the IEEE EMBS*, volume 26 I, pages 4009–4012, San Francisco, CA, USA, Sept. 2004.

[19] C. Vargas-Irwin and J. P. Donoghue. Automated spike sorting using density grid contour clustering and subtractive waveform decomposition. *Journal of neuroscience methods*, 164(1):1–18, August 2007.

[20] J. S. Prentice, J. Homann, K. D. Simmons, G. Tkačik, V. Balasubramanian, and P. C. Nelson. Fast, scalable, Bayesian spike identification for multi-electrode arrays. *PLoS ONE*, 6(7):e19884, 07 2011.

[21] D. Novak, J. Wild, T. Sieger, and R. Jech. Identifying number of neurons in extracellular recording. In *4th Annual International Conference of the IEEE Engineering in Medicine and Biology Society on Neural Engineering*, pages 742–745, Antalya, Turkey, 2009.

[22] C. Fraley and A. E. Raftery. How many clusters? Which clustering method? Answers via model-based cluster analysis. *The Computer Journal*, 41:578–588, 1998.

[23] Z. Tiganj and M. Mboup. A non-parametric method for automatic neural spikes clustering based on the non-uniform distribution of the data. *J. Neural Eng.*, 8(6):066014, 2011.

[24] Y. Shiraishi, N. Katayama, T. Takahashi, A. Karashima, and M. Nakao. Multi-neuron action potentials recorded with tetrode are not instantaneous mixtures of single neuronal action potentials. *Annual International Conference of the IEEE Engineering in Medicine and Biology Society.*, pages 4019–4022, 2009.

[25] G. D. Brown, S. Yamada, and T. J. Sejnowski. Independent component analysis at the neural cocktail party. *Trends in Neuroscience*, 24(1):54–63, January 2001.

[26] S. Takahashi, Y. Anzai, and Y. Sakurai. Automatic sorting for multi-neuronal activity recorded with tetrodes in the presence of overlapping spikes. *Journal of neurophysiology*, 89(4):2245–2258, April 2003.

[27] P. Comon and C. Jutten. *Handbook of Blind Source Separation, Independent Component Analysis and Applications.* Academic Press (Elsevier), 02 2010.

[28] A. Hyvärinen and E. Oja. Independent component analysis: algorithms and applications. *Neural Networks*, 13(4-5):411–430, 06 2000.

[29] C. Bedard, H. Kroger, and A. Destexhe. Modeling extracellular field potentials and the Frequency-Filtering properties of extracellular space. *Biophysical Journal*, 86(3):1829–1842, 2004.

[30] K. D. Harris, D. A. Henze, J. Csicsvari, H. Hirase, and G. Buzsáki. Accuracy of tetrode spike separation as determined by simultaneous intracellular and extracellular measurements. *Journal of Neurophysiology*, 84:401–414, Jul 2000.

[31] Pettersen K.H., Linden H., Dale A.M., and Einevoll G.T. Extracellular spikes and current-source density. *in Handbook of Neural Activity Measurement, edited by R. Brette and A. Destexhe, Cambridge*, 2012.

[32] M. Mboup. A Volterra filter for neuronal spike detection. *Research report, INRIA, http://hal inria fr/inria-00347048/en/*, 2008.

[33] L. Citi, J. Carpaneto, K. Yoshida, K.P. Hoffmann, K.P. Koch, P. Dario, and S. Micera. Characterization of tflife neural response for the control of a cybernetic hand. In *Biomedical Robotics and Biomechatronics, 2006. BioRob 2006. The First IEEE/RAS-EMBS International Conference on*, pages 477 –482, 2006.

[34] Citi L., Carpaneto J., Yoshida K., Hoffmann K.P., Koch K.P., Dario P., and Micera S. On the use of wavelet denoising and spike sorting techniques to process electroneurographic signals recorded using intraneural electrodes. *Journal of Neuroscience Methods*, 172(2):294 – 302, 2008.

[35] J. Thomas, Y. Deville, and S. Hosseini. Time-domain fast fixed-point algorithms for convolutive ICA. *Signal Processing Letters, IEEE*, 13(4):228 – 231, 2006.

[36] M. Dyrholm, S. Makeig, and L. K. Hansen. Model selection for convolutive ICA with an application to spatio-temporal analysis of EEG. *Neural Computation*, 2006.